

UC Office of the President

Recent Work

Title

Scalable Total Synthesis, IP3R Inhibitory Activity of Desmethylxestospongine B, and Effect on Mitochondrial Function and Cancer Cell Survival

Permalink

<https://escholarship.org/uc/item/46n9603r>

Author

Zakarian, Armen

Publication Date

2021-04-01

Peer reviewed

Total Synthesis

Scalable Total Synthesis, IP3R Inhibitory Activity of Desmethylxestospongine B, and Effect on Mitochondrial Function and Cancer Cell Survival

Maša Podunavac, Artur K. Mailyan, Jeffrey J. Jackson, Alenka Lovy, Paula Farias, Hernan Huerta, Jordi Molgó, Cesar Cardenas,* and Armen Zakarian*

Abstract: The scalable synthesis of the oxaquinolizidine marine natural product desmethylxestospongine B is based on the early application of Ireland–Claisen rearrangement, macrolactamization, and a late-stage installation of the oxaquinolizidine units by lactam reduction. The synthesis serves as the source of material to investigate calcium signaling and its effect on mitochondrial metabolism in various cell types, including cancer cells.

Xestospongins, along with araguspongins, are a group of natural products isolated from marine sponges of *Xestospongia* sp.^[1] Structurally, these compounds are comprised of two oxaquinolizidine units tethered by saturated alkylidene chains to form a macrocyclic core, and have variable oxidation and stereochemistry at C9/C9' (Figure 1).^[1] While a range of biological activity was reported for xestospongins, we became intrigued by the mounting evidence for the unique ability of xestospongine B to influence mitochondrial metabolism by modulating calcium signaling between the endoplasmic reticulum (ER) and mitochondria through the inhibition of inositol-1,4,5-triphosphate receptors (IP3Rs).^[2] The constitutive activity of IP3Rs is essential for cellular bioenergetics in a variety of cell types. Its inhibition disrupts the constitutive calcium transfer from ER to mitochondria causing a drop in mitochondrial respiration that generates a bioenergetic crisis characterized by AMPK and autophagy

How to cite: *Angew. Chem. Int. Ed.* **2021**, *60*, 11278–11282

International Edition: doi.org/10.1002/anie.202102259

German Edition: doi.org/10.1002/ange.202102259

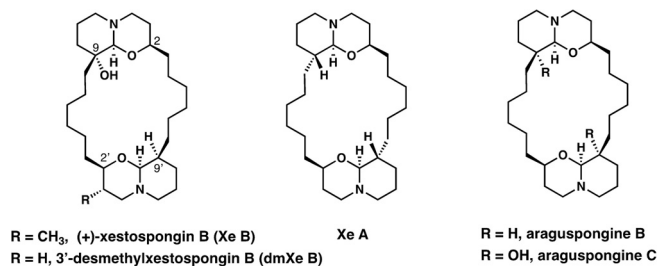


Figure 1. Structures of representative 1-oxaquinolizidine alkaloids.

activation.^[3] It has been shown that interruption of this communication leads to a selective, substantial cancer cell death leaving normal cells unaffected.^[4] One of the goals of this study was to evaluate the effect of desmethylxestospongine B on mitochondrial respiration in breast cancer cell lines, and the resultant selectivity in inducing cancer cell death leaving normal cells nearly unaffected.

While xestospongine B (XeB) is no longer available from the natural sources, total synthesis provides a feasible source of material. We targeted desmethylxestospongine B (dmXeB),^[1b] a natural product within this family of metabolites, based on the premise that the 3'-methyl group has no effect on the IP3R inhibitory activity, and obviating the need to install it would simplify the development of a scalable synthesis. While XeC and ArB are more accessible, they show lower specificity with notable side-effects on calcium homeostasis, and no data is available for ArC.^[2b]

Previous syntheses in this area by Baldwin^[5] and Hoye^[6] are characterized by remarkable brevity and strategic elegance, targeting C₂-symmetrical, non-hydroxylated congeners such as araguspongine B (ArB), and XeC and A, and resolving controversy about the absolute configuration of these compounds. However, the simplifying C₂-symmetry is broken in the biologically more intriguing XeB and dmXeB by the presence of 9-OH and, in the former case, the 3'-CH₃ groups.

The synthesis design is depicted in Scheme 1. The final assembly of the 1-oxaquinolizidine units was envisioned to take place by intramolecular *N*-alkylation of the amide groups in macrocyclic bis(lactam) **1** followed by lactam semireduction and hemiaminal formation. The bis(lactam) was planned to arise from combining two ω-amino acid precursors **2** and **3** by sequential amide formation. These precursors will be prepared from a common starting material, azidoalcohol **4**. After its esterification with either 2-(benzyloxy)-5-chloropentanoic acid (**5**) or 5-chloropentanoic acid,

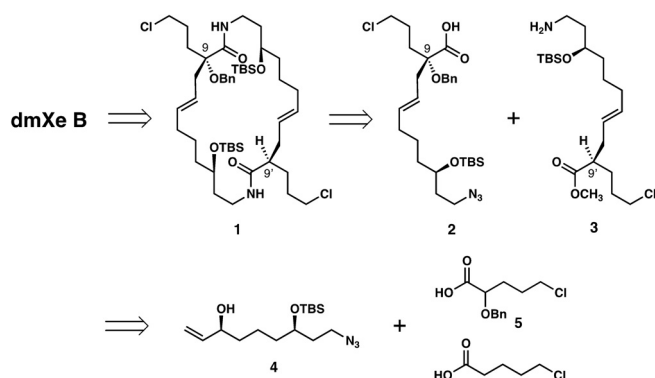
[*] M. Podunavac, Dr. A. K. Mailyan, Dr. J. J. Jackson, Prof. Dr. C. Cardenas, Prof. Dr. A. Zakarian
Department of Chemistry and Biochemistry
University of California Santa Barbara
Santa Barbara, CA 93106 (USA)
E-mail: zakarian@chem.ucsb.edu

Dr. A. Lovy, P. Farias, H. Huerta, Prof. Dr. C. Cardenas
Center for Integrative Biology, Faculty of Sciences, Geroscience
Center for Brain Health and Metabolism, Universidad Mayor
Santiago (Chile)
E-mail: julio.cardenas@umayor.cl

J. Molgó
Université Paris-Saclay, CEA, Institut des Sciences du Vivant Frédéric
Joliot, ERL CNRS n 9004, Département Médicaments et Technologies
pour la Santé, Service d'Ingénierie Moléculaire pour Santé (SIMoS)
Batiment 152, Point courrier 24, 91191 Gif-sur-Yvette (France)

Prof. Dr. C. Cardenas
The Buck Institute for Research on Aging
Novato, CA (USA)

Supporting information and the ORCID identification number(s) for the author(s) of this article can be found under <https://doi.org/10.1002/anie.202102259>.



Scheme 1. Synthesis design for dmXe B.

intermediates **2** and **3** will be accessed via Ireland-Claisen rearrangement to establish stereogenic centers at C9' and C9, respectively.

This synthesis design has the advantage of flexibility in accessing 1-oxaquinolizidine alkaloids with variable substitution at C9/9' (with or without OH groups), as well as variable stereochemistry at the same positions.

1-Chloro-3-butene served as the starting point for the synthesis of **4** (Scheme 2a). Jacobsen hydrolytic kinetic resolution of 1-chlorobutene oxide, obtained by epoxidation with MCPBA, delivered (*S*)-**6** in 58% yield and 92% *ee*.^[7] The epoxide was distributed divergently, with part of it being advanced to allylic alcohol **7** with dimethylmethylenesulfur ylide.^[8] After reductive *para*-methoxybenzyl (PMB) under electrophilic conditions and displacement of the chloro group, iodide **8** was obtained in a 71% overall yield.^[9] The development of electrophilic benzylation was required due to the propensity of **7** to undergo intramolecular etherification during alkoxide formation under a number of

reaction conditions. Cuprate coupling with the remainder of chloro epoxide (*S*)-**6** with the reagent formed from **8** was accomplished in 78% yield.^[10] Subsequent substitution of chloride with sodium azide, *O*-silylation, and removal of the PMB group delivered 58.1 grams of **4** in 87% yield.

In order to access non-symmetrical congeners such as dmXe B possessing a C9 hydroxy group, the synthesis of an α -benzyloxy acyl chloride **14** was required. Due to the thermal instability of ester enolates generated from α -alkoxy esters, alkylation of *t*-butyl α -benzyloxyacetate with iodide **10** was accomplished at -95°C in moderate yield of 45% under optimized reaction conditions. After desilylation, mesylation, and substitution with LiCl, ester **13** was obtained in 86% yield. Cleavage of the *t*-butyl ester and chlorohydroxylation with oxalyl chloride completed the synthesis of acyl chloride **14** (93% yield, 10.2 grams).

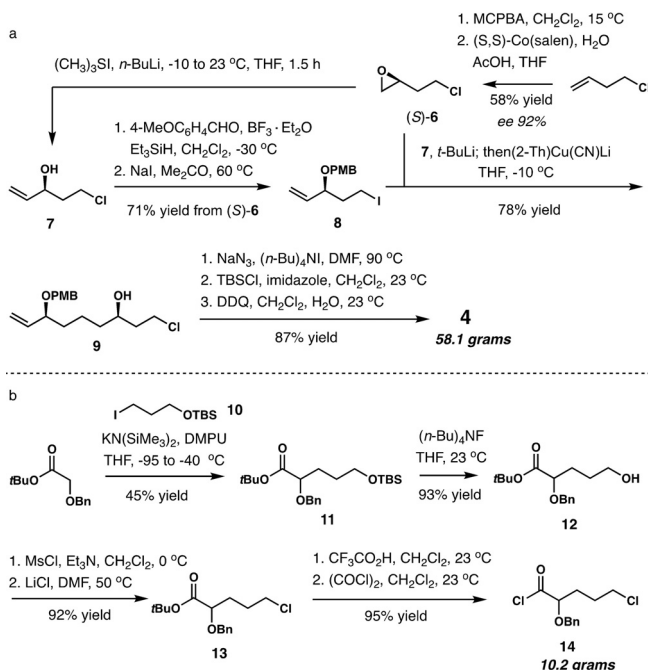
In preparation for the bis(macrolactam) assembly, the individual amino acid synthons were obtained by Ireland-Claisen rearrangement (ICR) of two esters prepared from allylic alcohol **4** (Scheme 3a and b).^[11] Intermediate **2** was obtained from ester **15** (82% yield, dr 10:1) under reaction conditions developed specifically for α -alkoxy esters, where we found that the best chelation-controlled outcome is achieved with KN(SiMe₃)₂/PhMe combination, while, surprisingly, LDA/THF affords non-chelation controlled diastereomer with good selectivity, despite the expected higher propensity of lithium to coordinate with oxygen Lewis bases.^[12] ICR of ester **16** gave rise to carboxylic acid **17** (87% yield, dr 6:1), which, after forming the methyl ester with Me₃SiCHN₂, was advanced to amino ester **3** by azide reduction with SnCl₂/PhSH (82% yield).^[13]

Fragment union was achieved by amide formation from acid **2** and amine **3**, followed by another azide reduction under the same conditions, ester hydrolysis, and macro-lactamization.^[14] At this stage, the minor diastereomers formed during ICR were separable, and macrocyclic bis-(lactam) **1** was isolated in 35% yield as a single diastereomer.

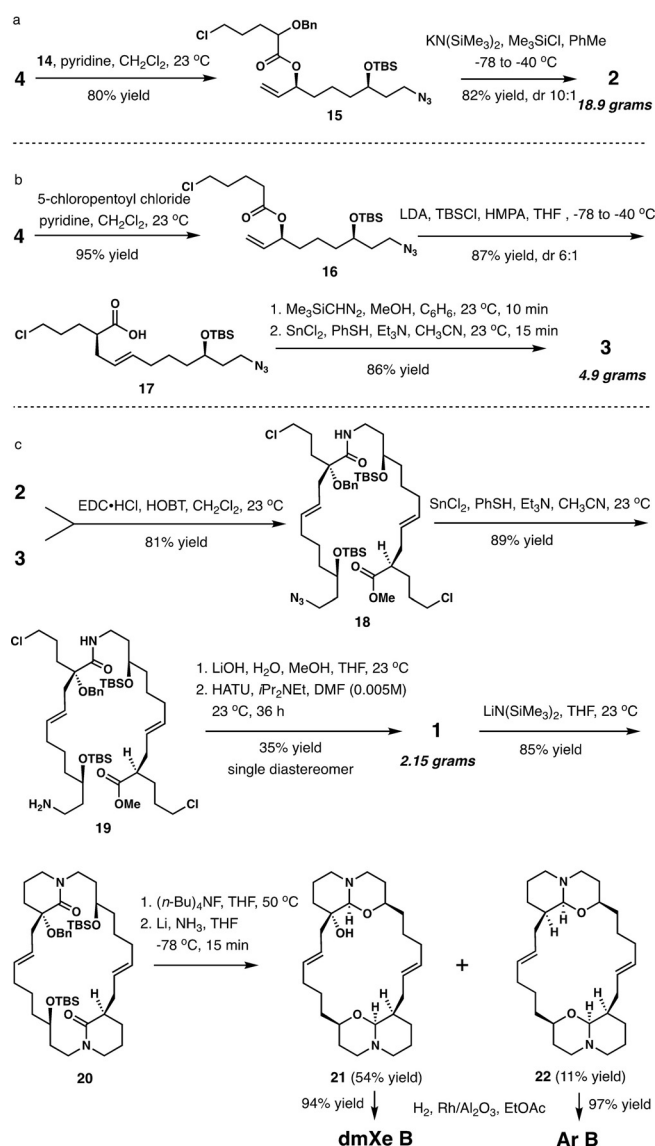
Completion of the synthesis follows a bidirectional strategy, starting with the formation of two valerolactam moieties by intramolecular *N*-alkylation of **1** (LiN(SiMe₃)₂, THF, 85% yield). Removal of the silyl groups preceded the crucial reductive 1-oxaquinolizidine formation with Li-NH₃ reagent, which simultaneously accomplished *O*-debenzylation.^[15] Notably, numerous alternative reagents attempted to achieve semireduction of the lactams (*i*Bu₂AlH,^[16] NaAlH₂(OR)₂,^[17] IrCl(CO)(PPh₃)₂/(HMe₂Si)₂O,^[18] consistently resulted in complete reduction to piperidine. Partial α -dehydroxylation leading to a minor amount of **22** was also observed.

The final hydrogenation of the double bonds required optimization, as the typical conditions using Pd/C in various solvents proved inconsistent and occasionally resulted in an intractable mixture of products. However, hydrogenation of **21** and **22** with Rh/Al₂O₃ in ethyl acetate^[19] reliably and cleanly delivered dmXe B (94% yield) and araguspongine B, (ArB, 97% yield), respectively.

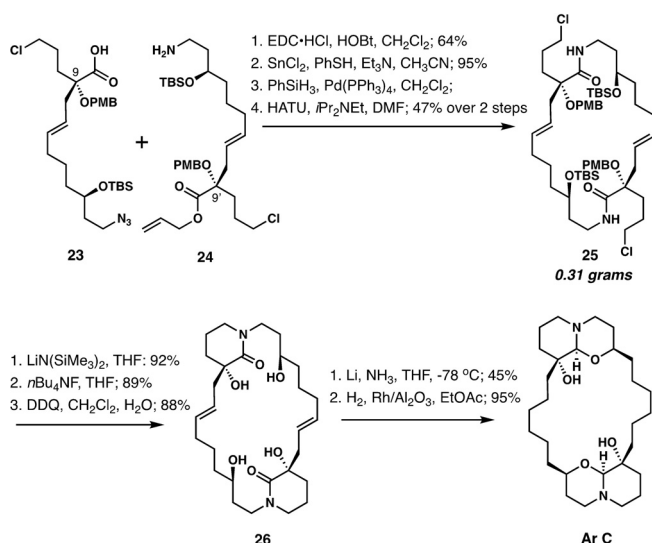
To further highlight the generality of the strategy, we completed the synthesis of bis-hydroxylated ArC, which has not been accessed previously by synthesis (Scheme 4, See Supporting Information for the synthesis of **23** and **24**). In this



Scheme 2. Preparation of early stage intermediates **4** and **14**.



Scheme 3. Fragment union and completion of the synthesis.



Scheme 4. The synthesis of araguspongine C (Ar C).

case, we opted for *p*-methoxybenzyl (PMB) ether at C9/9' to test an alternative deprotection/reductive oxaquinolizine construction method. We also utilized allyl ester in **24** to simplify access to the free acid, as the methyl ester proved resistant to hydrolysis. Thus, after acid **23** and amine **24** were combined by amide formation, azide reduction, acid deallylation, and macrolactamization afforded bis-lactam **25**. Six-membered lactam closure was accomplished with LiN(SiMe₃)₂ as previously, and removal of TBS and PMB groups delivered **26** in high yield. Finally, reduction of the lactam with Li-NH₃ and hydrogenation completed the synthesis of Ar C.

Having established access to synthetic dmXeB, we proceeded to evaluate its effect on IP3R-mediated calcium release, mitochondrial respiration and selective anticancer activity in breast cancer cell lines, and how it compares to XeB isolated previously from a marine sponge. As shown in Figure 2a, 30 min incubation with either dmXeB or XeB completely abolished IP3R calcium release induced by ATP in MDA-MB-231 cells. Subsequently, the normal cell line MCF10A and a cancer cell line MDA-MB-231 were treated with increasing concentrations of dmXeB and XeB for 24 h, and oxygen consumption rates (OCR) were determined using Seahorse system. As shown in Figure 2b, both compounds decrease OCR similarly in a dose-dependent fashion. A similar effect was observed in a triple-negative cell line BT-549 and the luminal A MCF7 cell line (See Supporting Information).

We have also demonstrated that dmXeB induces selective cell death in breast cancer cell lines. Several breast cancer cell lines that represent heterogeneity of breast cancer and the normal cell line MCF10A were treated with different concentrations of either XeB or dmXeB for 24 h and cell death was measured by propidium iodide incorporation through flow cytometry. As shown in Figure 2c, 7.5 μM XeB induced a significant increase in cell death in MDA-MB-231 cells, without affecting the normal cell line MCF10A. At 10 μM, XeB is still more effective in MDA-MB-231 cells, but some effects in MCF10A cells become measurable, indicating reduced selectivity. On the other hand, dmXeB in fact shows somewhat increase selectivity, inducing cell death in MDA-MB-231 at 5 μM, which is sustained at 10 μM with no effect on normal MCF10 cells (Figure 2c). At 20 μM, MDA-MB-231 cells are still more sensitive, with almost 100% of the population dead, whereas MCF10A shows an initial increase in cell death. In cell lines representative of luminal A (MCF7) and luminal B (ZR75) breast cancer cell lines XeB and dmXeB display selective cell death at concentrations between 5 and 10 μM. Similarly to the observations with MDA-MB-231 cell line, dmXeB at 20 μM concentration caused an almost complete cell death in ZR75 and MCF7 cell lines, while also affecting the normal cell line MCF10A to a much lesser extent. The BT-549 cells are more resistant to both compounds, showing only selectivity at 7.5 μM. Finally, we determined whether dmXeB affected the ability of cancer cells to proliferate indefinitely (one of the hallmarks of cancer), as demonstrated previously for XeB^[4] MDA-MB-231 cells were treated with either compound for 24 h and then one thousand cells were collected and reseeded. After one

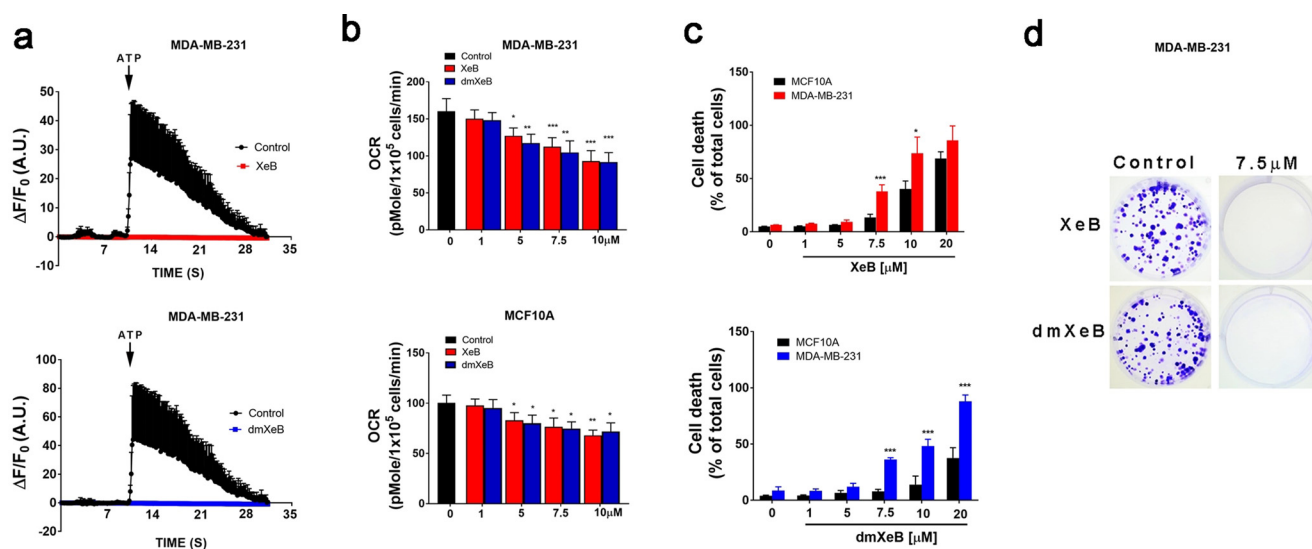


Figure 2. Average cytosolic calcium increases in response to ATP (100 μM) in MDA-MB-231 cells treated with ethanol (vehicle, control) or 5 μM XeB (upper panel, red trace) or dmXeB (bottom panel, blue trace) for 1 h. Mean \pm SEM of 3 independent experiments. In each experiment, 100 cells were analyzed. b) Basal oxygen consumption rate (OCR) of MDA-MB-231 (upper panel) and MCF10A (bottom panel) cells incubated for 24 h with increasing concentration of either XeB (red) or dmXeB (blue). The black bar represents cells basal OCR without treatment. Mean \pm SEM of 3 independent experiments with 10 replicates each. $*p < 0.05$, $**p < 0.01$, $***p < 0.001$ compared to respective control. c) MDA-MB-231 (upper panel) and MCF10A (lower panel) were treated with increasing concentrations of either XeB (upper panel, red) or dmXeB (lower panel, blue) for 24 h and cell death was determined by propidium iodide incorporation by flow cytometry. Mean \pm SEM of 3 independent experiments, each in triplicate. $*p < 0.05$, $***p < 0.001$ compared to respective control. d) Representative plates of three different experiments with MDA-MB-231 cells treated with 7.5 μM of either XeB (upper panel) or dmXeB (bottom panel).

week, we evaluated colony formation and found that at 7.5 μM the synthetic dmXeB, similarly to natural XeB, completely abolished this phenomenon (Figure 2d).

In summary, we developed a scalable synthesis of dmXeB, taking advantage of a convergent strategy allowing the preparation of xestospongins with variable stereochemistry and oxidation at C9/9', as attested to by the synthesis of ArC, which has not been accessed by previously described strategies. The hallmarks of the strategy include a strategic application of ICR to achieve the desired makeup of the C9/9' stereocenters, assembly of the macrocyclic core by macrolactamization, and late-stage 1-oxaquinolizidine construction by amide reduction. With dmXeB in hand, we established that it is an effective inhibitor of the constitutive ER-to-mitochondria calcium transfer, and subsequently confirmed its ability to induce selective cancer cell death in a variety of cell lines, including metastatic cancer, while leaving normal cells nearly unaffected. According to a recent study, these effects are associated with a drop in the mitochondrial activity of the calcium-sensitive α -ketoglutarate dehydrogenase, a key enzyme in oxidative phosphorylation and reductive carboxylation required for cancer cell survival.^[20]

Acknowledgements

This work was supported by ANID/FONDECYT grants 1160332 and 1200255, ANID/FONDAP grant 15150012 (C.C.), UC CRCC grant CRR-19-577249, and the NIGMS R01-077379 (A.Z.). MP is a recipient of the Tantiwawat

Fellowship, Mabe Memorial Fellowship, and UCSB Travel grant. We thank Dr. Hongjun Zhou for the assistance with the NMR spectrometry, Dr. Dmitri Uchenik for the assistance with mass spectrometry, and Dr. Guang Wu for the assistance with X-ray crystallography.

Conflict of interest

The authors declare no conflict of interest.

Keywords: cancer · IP3R receptor · metabolism · total synthesis · xestospongins

- [1] a) M. Nakagawa, M. Endo, N. Tanaka, L. Gen-Pei, *Tetrahedron Lett.* **1984**, 25, 3227–3230; b) S.-S. Moon, J. B. MacMillan, M. M. Olmstead, T. A. Ta, I. N. Pessah, T. F. Molinski, *J. Nat. Prod.* **2002**, 65, 249–254; c) M. Kobayashi, K. Kawazoe, I. Kitagawa, *Chem. Pharm. Bull.* **1989**, 37, 1676–1678; d) M. V. R. Reddy, D. J. Faulkner, *Nat. Prod. Lett.* **1997**, 11, 53–59; e) Y. Venkateswarlu, M. V. R. Reddy, J. V. Rao, *J. Nat. Prod.* **1994**, 57, 1283–1285; f) M. Kobayashi, M. Yasuhisa, S. Aoki, N. Murakami, I. Kitagawa, Y. In, T. Ishida, *Heterocycles* **1998**, 47, 195–203.
- [2] a) J. Gafni, J. A. Munsch, T. H. Lam, M. C. Catlin, L. G. Costa, T. F. Molinski, I. N. Pessah, *Neuron* **1997**, 19, 723–733; b) E. Jaimovich, C. Mattei, J. L. Liberona, C. Cardenas, M. Estrada, J. Barbier, C. Debitus, D. Laurent, J. Molgo, *FEBS Lett.* **2005**, 579, 2051–2057.
- [3] C. Cárdenas, R. A. Miller, I. Smith, T. Bui, J. Molgo, M. Müller, H. Vais, K. H. Cheung, J. Yang, I. Parker, C. Thompson, M. Birnbaum, K. R. Hallows, J. K. Foskett, *Cell* **2010**, 142, 270–283.

- [4] C. Cárdenas, M. Müller, A. McNeal, A. Lovy, F. Jaña, G. Bustos, N. Smith, J. Molgó, A. Diehl, T. W. Ridky, J. K. Foskett, *Cell Rep.* **2016**, *14*, 2313–2324.
- [5] J. E. Baldwin, A. Melman, V. Lee, C. R. Firkin, R. C. Whitehead, *J. Am. Chem. Soc.* **1998**, *120*, 8559–8560.
- [6] a) T. R. Hoye, J. T. North, L. J. Yao, *J. Am. Chem. Soc.* **1994**, *116*, 2617–2618; b) T. R. Hoye, Z. Ye, L. J. Yao, J. T. North, *J. Am. Chem. Soc.* **1996**, *118*, 12074–12081.
- [7] S. E. Schaus, B. D. Brandes, J. F. Larrow, M. Tokunaga, K. B. Hansen, A. E. Gould, M. E. Furrow, E. N. Jacobsen, *J. Am. Chem. Soc.* **2002**, *124*, 1307–1315.
- [8] L. Alcaraz, J. J. Hartnett, C. Mioskowski, J. P. Martel, T. Le Gall, D. S. Shin, J. R. Falck, *Tetrahedron Lett.* **1994**, *35*, 5449–5452.
- [9] Y. Morimoto, M. Iwahashi, K. Nishida, Y. Hayashi, H. Shirahama, *Angew. Chem. Int. Ed. Engl.* **1996**, *35*, 904–906; *Angew. Chem.* **1996**, *108*, 968–970.
- [10] B. H. Lipshutz, J. A. Kozlowski, D. A. Parker, S. L. Nguyen, K. E. McCarthy, *J. Organomet. Chem.* **1985**, *285*, 437–447.
- [11] a) R. E. Ireland, R. H. Mueller, A. K. Willard, *J. Am. Chem. Soc.* **1976**, *98*, 2868–2877; b) E. A. Iardi, C. E. Stivala, A. Zakarian, *Chem. Soc. Rev.* **2009**, *38*, 3133–3148.
- [12] M. Podunavac, J. J. Lacharity, K. E. Jones, A. Zakarian, *Org. Lett.* **2018**, *20*, 4867–4870.
- [13] M. Bartra, P. Romea, F. Urpi, J. Vilarrasa, *Tetrahedron* **1990**, *46*, 587–594.
- [14] A. El-Faham, F. Albericio, *Chem. Rev.* **2011**, *111*, 6557–6602.
- [15] a) K. M. Allan, B. M. Stoltz, *J. Am. Chem. Soc.* **2008**, *130*, 17270–17271; b) D. A. Evans, C. R. Illig, J. C. Saddler, *J. Am. Chem. Soc.* **1986**, *108*, 2478–2479.
- [16] a) S. Kim, K. H. Ahn, *J. Org. Chem.* **1984**, *49*, 1717–1724; b) K. H. Ahn, S. J. Lee, *Tetrahedron Lett.* **1992**, *33*, 507–510.
- [17] a) F. Roussi, J.-C. Quirion, A. Tomas, H.-P. Husson, *Tetrahedron* **1998**, *54*, 10363–10378; b) M. Amat, N. Llor, J. Hidalgo, C. Escolano, J. Bosch, *J. Org. Chem.* **2003**, *68*, 1919–1928.
- [18] a) A. W. Gregory, A. Chambers, A. Hawkins, P. Jakubec, D. J. Dixon, *Chem. Eur. J.* **2015**, *21*, 111–114; b) P. W. Tan, J. Seayad, D. J. Dixon, *Angew. Chem. Int. Ed.* **2016**, *55*, 13436–13440; *Angew. Chem.* **2016**, *128*, 13634–13638.
- [19] a) W. F. Berkowitz, S. C. Choudhry, J. A. Hrabie, *J. Org. Chem.* **1982**, *47*, 824–829; b) O. Golan, Z. Goren, S. E. Biali, *J. Am. Chem. Soc.* **1990**, *112*, 9300–9307.
- [20] C. Cardenas, A. Lovy, E. Silva-Pavez, F. Urrea, C. Mizzoni, U. Ahumada-Castro, G. Bustos, F. Jaña, P. Cruz, P. Farias, E. Mendoza, H. Huerta, P. Murgas, M. Hunter, M. Rios, O. Cerda, I. Georgakoudi, A. Zakarian, J. Molgó, J. K. Foskett, *Sci. Signaling* **2020**, *13*, eaay1212.

Manuscript received: February 13, 2021

Accepted manuscript online: March 10, 2021

Version of record online: April 8, 2021